

# RECENT ADVANCES AND NEW TECHNIQUES IN VISUALIZATION OF ULTRA-SHORT RELATIVISTIC ELECTRON BUNCHES\*

Dao Xiang<sup>†</sup>, SLAC, Menlo Park, CA, 94025, USA

## Abstract

We review recent advances in the measurement of ultra-short relativistic electron bunches. We will focus on several techniques and their variants that are capable of breaking the femtosecond time barrier in measurements of ultra-short bunches. Techniques for measuring beam longitudinal phase space as well as the x-ray pulse shape in an x-ray FEL are also discussed.

## INTRODUCTION

Ultrashort electron bunches with rms length of  $\sim 1$  femtosecond (fs) can be used to generate ultrashort x-ray pulses in FELs [1] that may open up many new regimes in ultra-fast sciences. It is also envisioned that ultrashort electron bunches may excite  $\sim$ TeV/m wake fields for plasma wake field acceleration and high field physics studies [2]. Recent success of using 20 pC electron beam to drive an x-ray FEL at LCLS [3] has stimulated world-wide interests in using low charge beam (1 $\sim$ 20 pC) to generate ultrashort x-ray pulses (0.1 fs  $\sim$  10 fs) in FELs.

Accurate measurement of the length (preferably the temporal profile) of the ultrashort electron bunch is essential for understanding the physics associated with the bunch compression and transportation. However, the shorter and shorter electron bunch greatly challenges the present beam diagnostic methods. In this paper we review the recent advances in the measurement of ultra-short electron bunches. We will focus on several techniques and their variants that provide the state-of-the-art temporal resolution. Methods to further improve the resolution of these techniques and the promise to break the 1 fs time barrier is discussed.

## STREAK CAMERA

Streak cameras are perhaps the most widely used equipments in time domain to measure electron bunch temporal profile. It uses a time-varying deflection to convert the temporal profile of a light pulse into a spatial profile. Limited by the initial spread of the photoelectrons and the available sweeping electric field, the state-of-the-art streak camera provides about 200 fs temporal resolution [4].

A straightforward way to improve the temporal resolution of a streak camera is to increase the sweeping electric field, i.e. using an rf cavity to sweep the photoelectrons. Another possible method is to lengthen the light pulse generated by the electron beam before it is measured with a

streak camera (the pulse shape needs to be preserved during the stretching process). However, implementation of these schemes will likely make the streak camera difficult to fit in a small table.

## TRANSVERSE CAVITY

A transverse cavity (TCAV) is an rf structure operating in transverse mode. When a beam passes through a TCAV at the zero-crossing phase, the TCAV imprints a transverse angular kick (here we assume the kick is in vertical direction) on the beam that varies linearly with the longitudinal position ( $y' \propto t$ ). After about 90 degrees phase advance, the angular distribution is converted to spatial distribution, and the vertical axis on some screen downstream of the TCAV becomes the time axis ( $y \propto t$ ). It is straightforward to show that the vertical beam size on the screen is,

$$\sigma_y = \sqrt{\sigma_{y0}^2 + r_{12}^2 k^2 \sigma_{z0}^2}, \quad (1)$$

where  $\sigma_{y0}$  is the beam size on the screen when the TCAV is off,  $k = 2\pi eV/\lambda_{rf} E$  is the dimensionless kick strength of the TCAV and  $r_{12}$  is the angular-to-spatial element of the transfer matrix from the TCAV to the screen. In order to unambiguously determine the temporal profile of the beam, one may require the beam size on the screen to be dominated by the kick imprinted in the TCAV. Therefore, the resolution ( $\Delta t = \sigma_y'/k$ ) is limited by the intrinsic beam emittance and the available dimensionless kick of the TCAV. Currently, TCAVs have achieved a resolution of 10 $\sim$ 20 fs in measuring ultrashort bunches [5, 6].

## Optical Oscilloscope

From Eq. (1) it is easy to realize that a stronger kick from the TCAV provides a higher temporal resolution. This can be achieved by increasing the voltage and frequency of the TCAV. For instance, given the same voltage, an X-band TCAV provides 4 times higher resolution than an S-band TCAV. An X-band TCAV with maximal voltage of about 50 MV will be installed in FY13 at LCLS to push the resolution to 1  $\sim$  2 fs [7].

It is also possible to dramatically increase the frequency of the streaking field, say  $\times 1000$ , for which case a laser operating in TEM01 mode is used as the optical deflector. Note, the fact that the kick is only constant around the zero-crossing limited the application of an optical deflector to the case where the bunch is much shorter than the laser wavelength. To improve the dynamic range of the measurement, an 'optical oscilloscope' has been recently proposed where in addition to an optical laser, a TCAV is used

\* Work supported by US DOE contracts DE-AC02-76SF00515.

<sup>†</sup> dxiang@slac.stanford.edu

to streak the beam in an orthogonal direction [8]. The outcome of such a configuration is a 2-D map which shows the overall bunch shape as well as the fine structures. In principle, with a high power laser the resolution of this method can be pushed to sub-femtosecond.

### Longitudinal-to-transverse Mapping

A more exotic way to improve the temporal resolution of a TCAV is to remove the  $\sigma_{y0}$  term in Eq. (1), namely, making the transverse beam distribution on the screen independent of the beam emittance. In [9] we have shown that by introducing a special chicane with non-zero  $R_{54}$  upstream of the TCAV, particle's initial longitudinal position can be exactly mapped to the final transverse position, which overcomes the fundamental resolution limit arising from the beam intrinsic emittance. The resolution of this mapping technique is only limited by second order effects. The technique has been applied to LCLS beam and about 0.2 fs resolution has been confirmed in simulation.

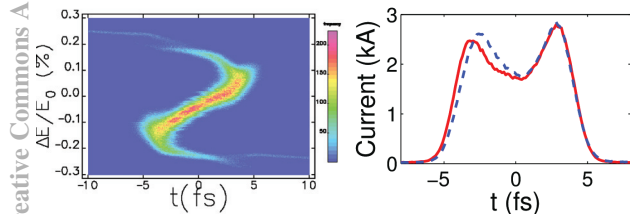


Figure 1: (Left) Longitudinal phase space for the under-compressed LCLS beam; (Right) True temporal profile (red) and predicted temporal profile (blue) from the longitudinal-to-transverse mapping technique (from Ref. [9]).

It's worth mentioning that a more universal method to map  $z$  exactly to  $y$  is through phase space exchange [10] where quadrupoles are added before and after an emittance exchange beam line to exchange the coordinates as well, i.e. mapping  $y$  to  $z$ ,  $y'$  to  $\delta$ ,  $z$  to  $y$ , and  $\delta$  to  $y'$ .

### Measure X-ray Temporal Profile

An TCAV together with an energy spectrometer allows a complete characterization of the beam longitudinal phase space. This configuration has been widely used in x-ray FEL facilities to reveal the beam longitudinal phase space such that one can tune the harmonic cavity to properly linearize the beam longitudinal phase space.

Recent studies show that one can also obtain the x-ray pulse shape in an FEL facility through measurement of the beam longitudinal phase space after the undulator [7]. The idea is rather simple: the FEL interaction in the undulator increases the beam energy spread and as a result the time-dependent beam energy loss and energy spread growth copies that of the x-ray pulse shape. Therefore, measurement of the beam longitudinal phase space after

the undulator and referencing it with the measurement with FEL off allows one to infer the x-ray pulse shape. One of the many advantages of this method is that it works at any x-ray wavelength as long as the energy spread growth from FEL interaction is much larger than the initial energy spread. The resolution is determined by the TCAV, and therefore could approach 1 fs. This method will be tested in LCLS soon.

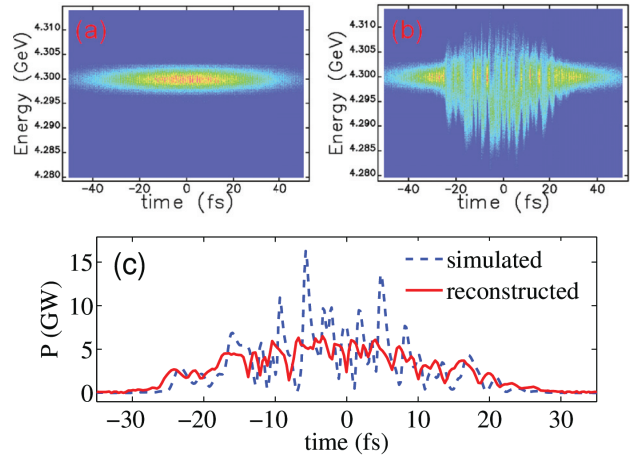


Figure 2: Beam longitudinal phase space with FEL off (a) and on (b); (c) X-ray power profile (provided by Y. Ding).

### Measure Energy Modulation

One drawback of the above method in measuring beam longitudinal phase space is that the transverse accelerating field in a TCAV will increase the beam slice energy spread, which contaminates the true beam energy distribution before it is measured in the energy spectrometer. The energy spread growth is due to the longitudinal electric field that varies linearly with transverse distance. Furthermore, if a stronger streak is used to achieve a higher temporal resolution, the energy resolution is worse. While this energy spread growth in some particular cases are desirable (see for example, suppression of harmonics and microbunching instability [11, 12]), it makes simultaneous accurate measurement of longitudinal distribution and energy distribution difficult.

Recently an all-optical method [13] to measure the time-dependent laser energy modulation which was required in many advanced beam manipulation technique with lasers has been demonstrated at SLAC's NLCTA. In this method, a chicane is used to convert the time-dependent energy modulation into time-dependent density modulation, which is measured with a TCAV to infer the laser energy modulation amplitude. Because with this method a particle's energy is converted into longitudinal position before the beam passes through the TCAV and the particles' longitudinal positions do not change in the TCAV, it is immune to both the transverse emittance and the transverse acceleration effects in the TCAV, allowing both high temporal resolution

and high energy resolution to be achieved simultaneously.

## ZERO-PHASING

The zero-phasing method is analogous to the bunch temporal profile measurement with a TCAV, except that a time-dependent energy kick is imprinted by an rf structure operating in the fundamental mode. Specifically, when a beam passes through an rf structure at the zero-crossing phase, the structure imprints an energy kick on the beam that varies linearly with the longitudinal position ( $\delta \propto t$ ). After passing through an energy spectrometer (assuming bending plane to be horizontal), the energy distribution is converted to spatial distribution, and the horizontal axis on some screen becomes the time axis ( $x \propto t$ ).

This method has been widely applied to many facilities to measure ultra-short bunch [14-17]. Recently, the method was used to visualize the density modulated electron beam from a temporally shaped photocathode drive laser in SDL [18]. This method is easy to implement and provides a high temporal resolution comparable to that from a TCAV. The ultimate resolution of this method is limited by the initial beam energy spread at the entrance to the rf structure.

### Longitudinal-to-energy Mapping

Even before the method was given the name ‘zero-phasing’ in [15], it was realized that the resolution limit arising from the initial beam energy spread could be overcome with a simple trick, namely sending the beam through a chicane before it enters the rf structure [19]. For such a beam line, the final longitudinal coordinates  $(z_1, \delta_1)^T$  is related to the initial coordinates  $(z_0, \delta_0)^T$  by,

$$\begin{bmatrix} z_1 \\ \delta_1 \end{bmatrix} = \begin{bmatrix} 1 & 0 \\ h & 1 \end{bmatrix} \begin{bmatrix} 1 & R_{56} \\ 0 & 1 \end{bmatrix} \begin{bmatrix} z_0 \\ \delta_0 \end{bmatrix}. \quad (2)$$

It turns out by properly choosing the chicane strength and the voltage of the rf structure such that  $1 + hR_{56} = 0$ , one can map  $z_0$  exactly to  $\delta_1$ . Under this condition, we have  $z_0 = \delta_1/h$ . This is similar to the trick used in the longitudinal-to-transverse mapping [9] where a special chicane with non-zero  $R_{54}$  is used to improve the temporal resolution.

This longitudinal-to-energy mapping technique has been used in an FEL oscillator to measure the micro-bunches equally separated by  $60 \mu\text{m}$  [20]. Recently, it has been applied in LCLS to measure the ultra-short electron bunch [21, 22]. In the LCLS measurement, nearly 1 km S-band rf structure was used to streak the beam. This together with an energy spectrometer that has unusually high dispersion ( $\eta \approx 6 \text{ m}$ ) leads to a superb temporal resolution which confirms that an ultra-short bunch with rms length of about 1 fs can be generated in LCLS when it operates in the low charge mode. To the author’s knowledge, this is the shortest bunch resolved in time domain.

Recent analysis [23] shows that this longitudinal-to-energy mapping technique may even allow one to visualize the optical micro-bunches in inverse FELs and seeded

FELs. When a laser interacts with an electron beam in an undulator, it will generate energy modulation in beam phase space. After passing through a chicane, the energy modulation is converted into density modulation. As a result of this transformation, the beam that initially has a smooth distribution now consists of many bumps equally separated by the laser wavelength. Characterizations of these optical micro-bunches are typically carried out in frequency domain where the coherent radiation at the laser frequency and its harmonics are measured [24]. Direct visualization of these micro-bunches undoubtedly will provide new insights into the underlying physics and will have profound implications for seeded FELs.

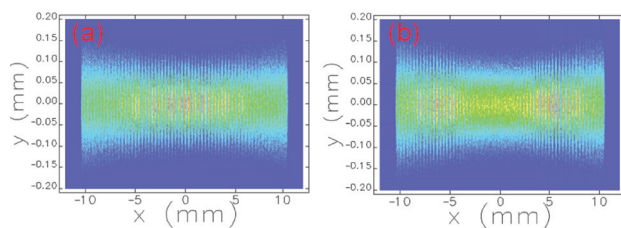


Figure 3: Simulated beam images for 5 keV energy modulation (a) and 12 keV energy modulation (b). Horizontal axis represents time.

Currently, a program called Echo-75 [25], which is an extension of the Echo-7 project [11, 24], is being planned at SLAC’s NLCTA. With a new X-band rf structure installed following the echo beam line, the optical micro-bunches may be directly visualized in time domain. Simulation using realistic parameters have confirmed the feasibility, as shown in Fig. 3. In the simulation, the optimal energy modulation that maximizes the bunching is around 5 keV. As shown in Fig. 3a, only the central part of the beam where it sees the peak modulation is perfectly bunched. As we increase the peak energy modulation to 12 keV, the beam in the central part is overbunched and those in the head and tail are optimally bunched. The slow oscillation of the bunching factor can be seen with a TCAV, similar to that reported in [13]. Here with the superb resolution from the longitudinal-to-energy mapping technique, the fast oscillation of the density modulation is unveiled as well. An experiment to test this is scheduled in early 2013.

## FREQUENCY DOMAIN METHODS

The methods in time domain discussed above provide unambiguous measurement of the beam temporal profile. However, the high accuracy is achieved at the price of high cost. Alternatively, the ultra-short bunch may be indirectly measured in frequency domain by measuring the spectrum of the bunch with a spectrometer or an interferometer that are less expensive. The measured spectrum of the radiation can be used to estimate the bunch length. With some phase retrieval algorithm, the temporal shape of bunch may be reconstructed from the spectrum as well [26].

## Interferometer

Michelson interferometer [27, 28] and Martin-Puplett interferometer [29, 30, 31] have been widely used to obtain the beam longitudinal distribution through measurement of the coherent radiation (synchrotron radiation, edge radiation, transition radiation, diffraction radiation, Smith-Percell radiation, etc.). The interferometer typically works in a multi-shot mode in which the radiation is split with a beam splitter and recombined to a detector. The measured energy as a function of path length difference of the split radiation is called the autocorrelation function of which the Fourier transform gives the radiation power spectrum.

Single-shot interferometer which combines the split radiation with an angle has also been developed and tested [32, 33]. Similar to the single-shot autocorrelators widely used for measuring laser pulse width, the radiation is combined with a small angle such that the angle correlates with the path length difference and a detector array can be used to measure the autocorrelation function in a single shot.

It is worth mentioning that an exotic interferometer, so-called beam-splitter-free interferometer, has been recently proposed to measure ultra-shot electron bunch [34]. In this technique, the beam first goes through an OTR foil to generate coherent transition radiation which further propagates downstream. After being delayed in a chicane, the beam goes through a second foil. When the delay of the chicane is shorter than the bunch duration, stimulated absorption of transition radiation will occur at the second foil because of the presence of the radiation field generated in the first foil. Variation in radiation intensity as a function chicane delay is only observed when the two radiation overlap in time, so the approximate bunch length can be easily obtained.

## Spectrometer

With a dispersive element (i.e. grating), the radiation spectrum within some spectral range can be measured in a single-shot. Recently, a multi-channel spectrometer based on 5 consecutive blazed reflection gratings has been built at DESY [35]. The layout of this device is shown in Fig. 4a where each grating disperses the radiation in the range  $\lambda_i \pm 0.25\lambda_i$  while reflects the lower frequency component of which the wavelength is longer than  $1.3\lambda_i$ , where  $i = (1, 2, 3, 4, 5)$ .

With 5 gratings with variant groove spacing, this device allows one to measure a wide range of wavelength. The results from two interchangeable sets that consist of 5 consecutive gratings and 120 line detectors are shown in Fig. 4b ('THz short' to cover  $5 \sim 44 \mu\text{m}$  and 'THz long' to cover  $45 \sim 400 \mu\text{m}$ ). The result is in good agreement with that obtained with a TCAV, especially in the long wavelength region. In the short wavelength region, the measured spectral intensity is generally larger than that inferred from TCAV measurement, which might indicate that the bunch has fine structures that are not resolved with the TCAV.

Similarly, with a grating and a prism, the radiation spectrum from a beam generated in a laser wake field accelera-

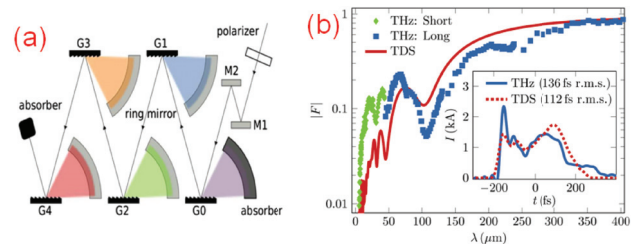


Figure 4: (a) Layout of the single-shot spectrometer; (b) Measured beam form factor from the spectrometer and that derived from measurement with a TCAV; the inset shows the beam temporal profile reconstructed from the spectrum and that from a TCAV (from [36]).

tor (LWFA) was measured in the range from about  $0.5 \mu\text{m}$  to  $5.5 \mu\text{m}$  [37]. Based on the measured radiation spectrum, an rms bunch length of about 1.5 fs was inferred. Strictly speaking, measurement of the spectrum in such a limited range neither precludes the existence of a longer bunch preceding or following the seemingly short bunch, nor does it exclude the possibility of a long bunch with a sharp peak with a width on the order of a few fs. However, with a hypothesis that the beam needs to be shorter than at least 1/4 of the plasma wavelength to get a decent energy spread and based on the fact that the plasma wavelength is on the order of  $\sim 10 \mu\text{m}$ , the conclusion that an ultra-short electron bunch can be routinely generated in a LWFA can still be drawn.

## LASER-BASED METHODS

Using lasers to measure electron beam parameters may date back to 1960's when inverse Compton scattering was suggested to measure plasma parameters. Later in the 1990's the inverse Compton scattering technique was used to measure bunch length [38] for a relativistic electron beam generated in accelerators. In the last decade, extensive efforts have been devoted to developing laser-based methods for characterization of ultra-short bunches and we expect these efforts to continue in the future.

### Electro-optical Sampling (EOS)

The idea of using EOS to measure electron beam longitudinal distribution is that for relativistic electron beam the Coulomb field copies that of the beam temporal profile. Specifically, when a laser propagates in an EO crystal, its polarization changes with the presence of an electric field carried by the electron beam. This field-induced birefringence results in a temporal or spectral changes of the laser, which can be used to infer the bunch temporal profile.

Since the first implementation of this technique in a multi-shot mode for measuring electron bunch profile [39], several variants of this technique have been demonstrated in the last decade that extends the EOS to single-shot mode and greatly improves the temporal resolution as well

[40, 41, 42]. Now EOS is routinely used for measurement of electron bunch profile and for recording the electron-laser timing jitter. The resolution of EOS for low energy beam is typically limited by the finite opening angle of the Coulomb field to  $2R/\gamma$ , where  $R$  is the distance from the crystal to the electron beam and  $\gamma$  is the relativistic factor. For high energy beam, the resolution is mainly limited by the response bandwidth of the crystals. The results of EOS are benchmarked with those from a TCAV and the highest resolution with EOS achieved so far is about 50 fs [43]. Very recently, a new method called bandwidth mixing FROG has been proposed [44] which may extend the resolution of EOS to about 10 fs.

### Optical Replica Synthesizer (ORS)

In the ORS scheme [45], a laser is used to generate density modulation in electron beam that is further sent through an undulator to generate intense radiation at the carrier frequency of the seed laser. Analysis shows that the field of the radiation is a replica of the beam temporal profile. The biggest advantage of ORS is that both the field and frequency of the radiation can be measured with frequency-resolved optical gating (FROG) technique well established in laser community [46], which can be used to obtain the temporal profile and energy chirp of the beam.

A proof-of-principle experiment in FLASH provided encouraging results [47]. While the FROG technique has been successfully used to measure a 4.5 fs laser pulse, the slippage length in the radiator undulator ultimately limited the resolution of ORS. This is because implementation of the FROG technique in a single-shot mode typically requires  $> 1 \mu\text{J}$  radiation energy which requires an undulator with several number of periods. This will limit the temporal resolution to a few tens of femosecond and it also make it difficult to use ORS to measure electron beam with low or moderate current.

Recently, a simplified version of ORS has been proposed [48]. In this scheme, the radiator undulator is replaced with an OTR screen and only the radiation spectrum needs to be measured. This scheme is easy to implement and does not require generation of high-power radiation for FROG measurement, yet still allows the rms length of an ultrashort bunch to be obtained. In this scheme, the COTR spectrum will be measured to infer the bunch length.

## REFERENCES

- [1] S. Reiche *et al.*, Nucl. Instrum. Methods Phys. Res., Sect. A 593, 45 (2008).
- [2] J. Rosenzweig *et al.*, Nucl. Instrum. Methods Phys. Res., Sect. A 653, 98 (2011).
- [3] Y. Ding *et al.*, Phys. Rev. Lett, 102, 254801 (2009).
- [4] M. Uesaka *et al.*, Nucl. Instrum. Methods Phys. Res., Sect. A 406, 371 (1998).
- [5] G. Berden *et al.*, Phys. Rev. Lett, 99, 164801 (2007).
- [6] K. Bane *et al.*, Phys. Rev. ST Accel. Beams, 12, 030704 (2009).
- [7] Y. Ding *et al.*, Phys. Rev. ST Accel. Beams, 14, 120701 (2011).
- [8] G. Andonian *et al.*, Phys. Rev. ST-AB 14, 072802 (2011).
- [9] D. Xiang and Y. Ding, Phys. Rev. ST Accel. Beams, 13, 094001 (2010).
- [10] D. Xiang and A. Chao, Phys. Rev. ST-AB 14, 114001 (2011).
- [11] D. Xiang *et al.*, Phys. Rev. Lett. 108, 024802 (2012).
- [12] C. Behrens *et al.*, Phys. Rev. ST-AB 15, 022802 (2012).
- [13] D. Xiang *et al.*, Phys. Rev. ST-AB 14, 112801 (2011).
- [14] X.J. Wang *et al.*, Phys. Rev. E 54, R3121 (1996).
- [15] D.X. Wang *et al.*, Phys. Rev. E 57, 2283 (1998).
- [16] W. Gaves *et al.*, Proceedings of PAC01, p2224 (2001).
- [17] D. Xiang *et al.*, Proceedings of IPAC10, p2299 (2010).
- [18] Y. Shen *et al.*, Phys. Rev. Lett. 107, 204801 (2011).
- [19] E.R. Crosson *et al.*, AIP Conf. Proc. No. 367, p397 (1996).
- [20] K. Ricci and T. Smith, Phys. Rev. ST-AB 3, 032801 (2000).
- [21] Z. Huang *et al.*, Phys. Rev. ST-AB 13, 092801 (2010).
- [22] Z. Huang *et al.*, Proc. of PAC11, p2459 (2011).
- [23] D. Xiang *et al.*, *Visualizing optical-mirobunches*, unpublished (2012).
- [24] D. Xiang *et al.*, Phys. Rev. Lett. 105, 114801 (2010).
- [25] E. Hemsing, Proc. of FLS12, (2012).
- [26] R. Lai and A. Sievers, Phys. Rev. E 50, R3342 (1994).
- [27] P. Kung *et al.*, Phys. Rev. Lett. 73, 967 (1994).
- [28] A. Lumpkin *et al.*, Nucl. Instrum. Methods Phys. Res., Sect. A 475, 470 (2001).
- [29] A. Murokh *et al.*, Nucl. Instrum. Methods Phys. Res., Sect. A 410, 452 (1998).
- [30] M. Castellano *et al.*, Phys. Rev. E 63, 056501 (2001).
- [31] D. Xiang *et al.*, Chinese Phys. Lett. 25, 2440 (2008).
- [32] G. Andonian *et al.*, Proc. of IPAC10, p1212 (2010).
- [33] J. Thangaraj *et al.*, Rev. Sci. Instru. 83, 043302 (2012).
- [34] D. Xiang *et al.*, *A beam-splitter-free interferometer for measuring ultra-short electron bunch*, unpublished (2012).
- [35] S. Wesch *et al.*, Nucl. Instrum. Methods Phys. Res., Sect. A 665, 40 (2011).
- [36] C. Behrens *et al.*, Phys. Rev. ST-AB 15, 030707 (2012).
- [37] O. Lundh *et al.*, Nature Phys., 7, 219 (2011).
- [38] W. Leemans *et al.*, Phys. Rev. Lett. 77, 4182 (1996).
- [39] X. Yan *et al.*, Phys. Rev. Lett. 85, 3404 (2000).
- [40] I. Wilke *et al.*, Phys. Rev. Lett. 88, 124801 (2002).
- [41] G. Berden *et al.*, Phys. Rev. Lett. 93, 114802 (2004).
- [42] A. Cavalieri *et al.*, Phys. Rev. Lett. 94, 114801 (2005).
- [43] G. Berden *et al.*, Phys. Rev. Lett. 99, 164801 (2007).
- [44] M. Helle *et al.*, Phys. Rev. ST-AB 15, 052801 (2012).
- [45] E. Saldin *et al.*, Nucl. Instrum. Methods Phys. Res., Sect. A 539, 499 (2005).
- [46] R. Trebino, Nature Photon. 5, 189 (2011).
- [47] P. Salen *et al.*, Proc. of FEL09, p739 (2009).
- [48] D. Xiang, in proposal to DOE early career award, unpublished (2011).